Study of the Preparation and Properties of UV-Blocking Fabrics of a PET/TiO_2 Nanocomposite Prepared by In Situ Polycondensation

Keqing Han, Muhuo Yu

State Key Laboratory of Chemical Fibers and Polymer Materials, College of Material Science and Engineering, Donghua University, Shanghai 200051, People's Republic of China

Received 3 December 2004; accepted 12 July 2005
DOI 10.1002/app.23312
Published online in Wiley InterScience (www.interscience.wiley.com).

ABSTRACT: Poly(ethylene phthalate) (PET)/nano-TiO_2 composites prepared via *in situ* polymerization were spun into fiber by the melt-spinning process. The dispersion of nanosized rutile TiO_2 in the PET was studied using transmission electron microscopy (TEM) and scanning probe microscopy (SPM) techniques. The mechanical properties and the properties of ultraviolet (UV) protection were investigated. The results showed that rutile TiO_2 can be dispersed uniformly by the *in situ* polycondensation process. The mechanical properties of PET/TiO_2 fiber were slightly affected by adding nano-TiO_2. The UV-ray transmittance of PET/nano-TiO_2 fabrics was below 10% in the UV-A band and below 1% in the UV-B band. And the ultraviolet protection factor (UPF) of PET/nano-TiO_2 fabrics was greater than 50. All these PET/TiO_2 nanocomposite fabrics exhibited excellent UV-blocking properties. © 2006 Wiley Periodicals, Inc. J Appl Polym Sci 100: 1588–1593, 2006

Key words: nanocomposites; polyester; fibers; ultraviolet

INTRODUCTION

Ultraviolet (UV) radiation—UV-A, UV-B, and UV-C—falls into the regions 315–400, 280–315, and 200–280 nm, respectively. Small doses of UV solar radiation are beneficial to humans, but large doses of UV radiation have detrimental effects, such as sunburn, premature skin aging, even skin cancer and cataracts. Therefore, the skin needs to be protected from excessive UV radiation, primarily UV-B radiation, because it has the highest skin damage potential.[1–3]

To indicate protection from UV radiation, the term *sun protection factor* (SPF) is widely used, especially for cosmetic skin protection products. There are two methods used to determine SPFs: *in vivo* and *in vitro.*[2] Another term, *ultraviolet protection factor* (UPF), which is defined in Australian/New Zealand Standard AS/NZS 4399:1966,[4] has been widely adopted now. UPF is primarily used to evaluate the UV protection capacity of textile products. It is based on an *in vitro* test method.

The UV protection effect of a fabric depends on many factors such as type of substrate, fabric construction, and fabric color. To achieve and improve good skin protection, a UV absorber can be applied during polymerization, fiber manufacture, or the final finish process. For example, nanotitania (TiO_2) is a kind of UV absorber.

With the development of nanosized materials in recent years, the preparation and application of nanotitania has been paid more attention because it is a material of many excellent properties. As is known, titania exists in three forms: anatase, rutile, and brookite.[5] Of these three, brookite is stable only at very low temperature and hence is not useful in a practical sense.[6] Anatase has high photochemical activity and can degrade polymers under the action of UV radiation. Rutile shows many interesting characteristics, such as absorption of UV light up to the proximity of visible light wavelengths, transparency at visible light wavelengths, and a very high refractive index. Therefore, nanocomposites containing rutile may be of interest for the fabrication of visually transparent UV filters as well as for coatings for UV-sensitive materials and lenses.[6–8]

In the preparation of nanocomposites, the key issue is the dispersion of nanoparticles or eliminating the aggregation of nanoparticles. Many efforts have been made to solve this problem. The available methods include the sol–gel blending technique,[9] the melt-blending process,[10] the *in situ* polymerization process,[11–13] and the *in situ* forming nanoparticles process.[14] Among these methods, the *in situ*–forming nanoparticle process is the most reasonable and effective because it can produce single particle dispersion composites. However, the *in situ*–forming nanopar-

Correspondence to: M. Yu (yumuhuo@dhu.edu.cn).

TABLE I
Spinning Technical Parameters of PET/TiO_2 Nanocomposites

Section No.	Screw 1	Screw 2	Screw 3	Screw 4	Spinning pump	Spinning beam
Temperature (°C)	280	295	300	300	300	305

ticle process can only be used for those systems in which no transformation of the crystal morphology of nanoparticles is needed at high temperature because the matrix polymer usually cannot endure high temperature.

Thus, to improve the dispersion of rutile titania nanoparticles in the PET matrix, we developed an *in situ* polycondensation process to produce the PET/rutile titania nanocomposites. In this process the nanotitania was first treated with a coupling agent to introduce some organic functional groups onto the surface of the titania particles; then the nanoparticles were dispersed in ethylene glycol (EG); and, finally, EG reacted with terephthalic acid (PTA), thus going to polycondensation in the presence of titania nanoparticles to form PET/TiO_2 nanocomposites.

In this study, PET/TiO_2 nanocomposites prepared by *in situ* polymerization were spun into fiber. This polymerization method of PET nanocomposites could not only improve the spinnability of PET, but also improve the UV blocking of PET fibers because of the better dispersion of nano-TiO_2. At the same time, it could decrease the pressure of spinning pack and prolong its replacing period. The UV protection property of PET/nano-TiO_2 fiber was characterized by measuring the ultraviolet transmittance of the fabrics. The mechanical properties of PET/nano-TiO_2 fiber also were studied.

EXPERIMENTAL

Materials

PET/nano-TiO_2 composites containing different contents of rutile titania prepared by *in situ* polymerization were supplied by Shanghai Jiaotong University; rutile titania was treated with a silane coupling agent.

Transmission electron microscopy and scanning probe microscopy

The specimens were sectioned into roughly 100-nm layers. Transmission electron microscopy (TEM) photographs were obtained with an H-800 transmission electron microscope (Hitachi, Tokyo) operated at an accelerated voltage of 100 KV.

The specimens were pressed into films. Then a Nanoscope IV scanning probe microscope was employed to observe the dispersion of nano-TiO_2 in the PET matrix. The scanning scope of the probe was 5×5 μm in the X and Y directions and 2.5μm in the Z direction.

Polarizing microscope observation

The crystalline forms of the PET and PET/nano-TiO_2 samples were observed using a Japanese Olympus BX51 polarizing microscope. The samples were heated to 290°C at a heating rate of 130°C/min, kept for 3 min at 290°C to make them fully melt, and then cooled to 200°C at a cooling rate of 100°C/min.

Spinning of PET/TiO_2 nanocomposites

The PET/TiO_2 nanocomposites were spun into fiber with 36 monofilaments on an ABE-25 spinning machine at the take-up speed of 800 m/min; the temperatures in the screw region are listed in Table I. Then the drawing of fiber was carried out on a Barmag3013 drawing device at a temperature of 160°C with a draw ratio of 4.0.

Preparation of UV-blocking PET fabrics

PET fibers were woven into plain fabric on a hydraulic loom for measuring the UV radiation protection property of the fabric.

Characterization

Tensile test

The mechanical properties of PET/nano-TiO_2 fibers were measured using an AGS materials testing machine with a gauge length of 250 mm.

Fiber orientation measurements

Orientation factor of fiber was obtained using a model SCY-IV sound velocity measurement apparatus.

Crystallinity measurements

Wide-angle X-ray diffraction (WAXD) was carried out using a D/max-B X-ray diffractometer (Rigaku Co., Japan) in the reflection mode at 40 KV and 40 mA with

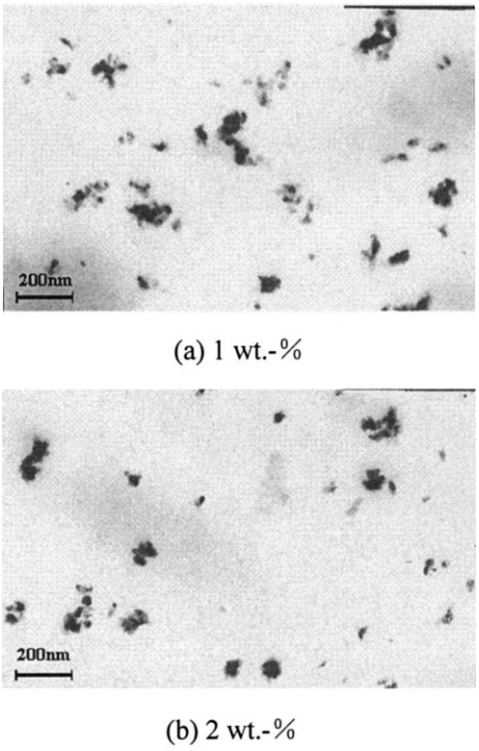

Figure 1 TEM images of sections of PET/TiO_2 nanocomposites with different TiO_2 contents.

a Cu target and Ni filter. The 2θ angle range was between 5° and 40°.

UV-blocking measurements

The UV ray transmittance of the PET fabrics was measured on a UV1000F ultraviolet spectrophotometer for characterizing the property of UV radiation protection of the fabrics.

RESULTS AND DISCUSSION

Figure 1 shows the TEM images of the PET/TiO_2 nanocomposites with different TiO_2 contents. As these images show, the TiO_2 particles were well dispersed in the polymer matrix. Although some TiO_2 particles aggregated in the matrix, the average particle diameter typically was below 100 nm.

Figure 2, which shows SPM photographs of PET/TiO_2 nanocomposites with different TiO_2 contents, further confirmed the dispersion of rutile in the composites.

In the polycondensation process, the nanotitania was first treated by a coupling agent to introduce some organic functional groups onto the surface of titania. Then the nanoparticles were dispersed in EG, a monomer of PET. Finally, EG reacted with PTA, going to polycondensation in the presence of titania nanoparticles to form PET/nanoparticle composites.

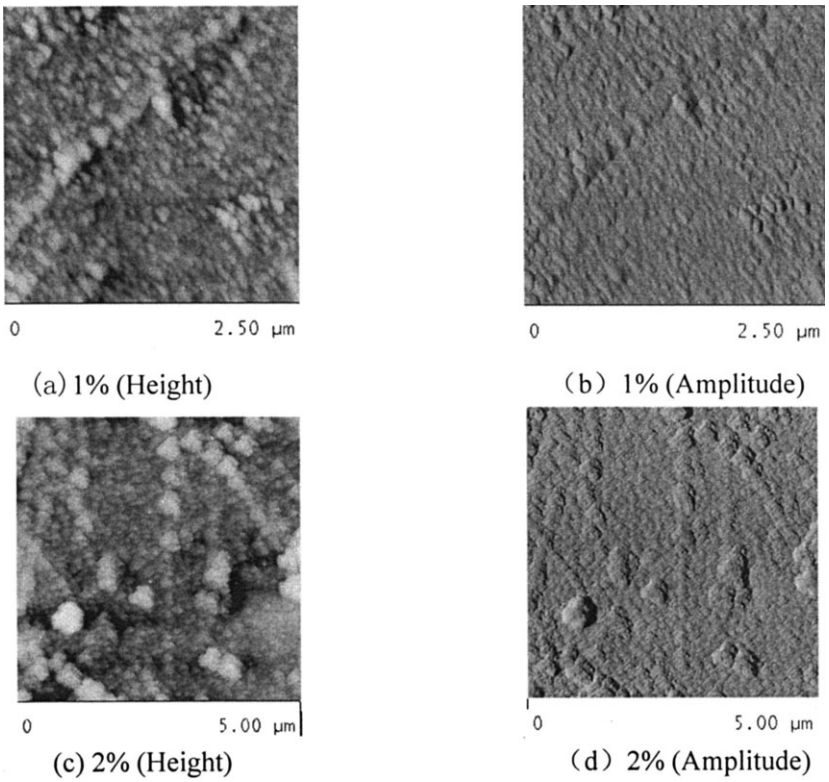

Figure 2 SPM images of PET/TiO_2 nanocomposites with different TiO_2 contents.

TABLE II
Mechanical Properties of PET/TiO_2 Fiber

Content of nano-TiO_2 (wt. %)	Tensile strength (MPa)	Elongation at break (%)	Modulus (GPa)	Orientation factor fs
0	514.74	34.47	12.64	0.88
1	483.00	27.10	12.76	0.91
2	459.54	30.53	12.45	0.88

In the spinning process the nanoparticles of the composites were first dispersed by shearing stress in the extruder and then were dispersed again by passing the spinning pack, which was filled by mesh- and sand filters. Therefore, nanoparticle aggregation was decreased to much less a degree, and its spinnability was better than that of composites prepared by melt blending. As compared with pure PET, the spinning parameters of PET/TiO_2 nanocomposites were similar. For example, the pressure of the spinning pack was kept at 42.5 kgf/cm^2, almost to the same as that of pure PET. During the spinning process, fiber breakage occurred very rarely.

The mechanical properties of PET/nano-TiO_2 fibers with different TiO_2 contents are listed in Table II. It can be seen that the tensile strength of the fiber with nano-TiO_2 decreased slightly. For example, the tensile strength of PET/nano-TiO_2 fiber with 1 wt % nano-TiO_2 decreased by about 6% compared with that of pure PET fiber. At the same time, the elongation at break of fiber decreased with the addition of TiO_2. It was assumed that the addition of nano-TiO_2 resulted in decreased interaction between the PET macromolecules. And the initial modulus and orientation factor of PET/TiO_2 fiber were kept almost the same as those of pure PET fiber.

Figure 3 shows the WAXD curves of fiber with different nano-TiO_2 contents. The crystallinity of fiber was calculated and is listed in Table III. It can be seen that the PET/nano-TiO_2 fiber had slightly lower crystallinity in comparison with pure PET fiber, which was coincident with the characteristics of the materials before spinning, as shown in the polarizing microscope images (see Fig. 4). A distinct, large spherulite in pure PET formed during the crystallization process, whereas only small-sized crystals appeared in the PET/TiO_2 nanocomposites. It is suggested that the TiO_2 nanoparticles dispersed in PET matrix acted as the nucleating agent in the PET crystallization process, which resulted in the formation of more imperfect microcrystals. At the same time, a greater number of crystal defects resulted in the decreased crystallinity of the fiber.

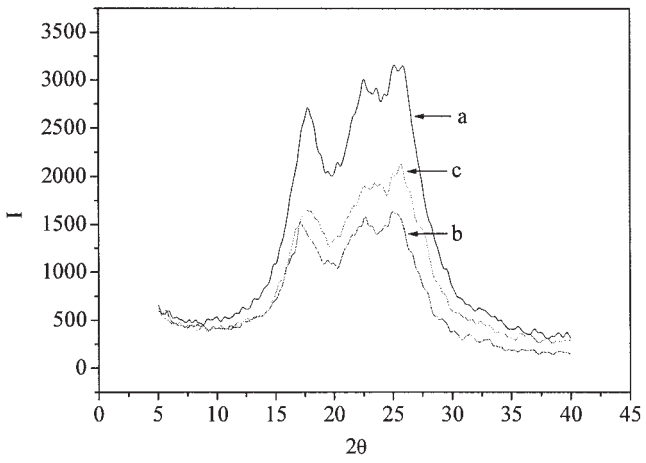

Figure 3 WAXD patterns of fibers with different nano-TiO_2 contents: (a) pure PET, (b) 1 wt % nano-TiO_2, (c) 2 wt % nano-TiO_2.

The UV-blocking mechanism of PET/nano-TiO_2 can be attributed to the electronic structure of nano-TiO_2, which can absorb light with an energy of $h\nu$, which matches or exceeds its band gap energy. The band gap energy of TiO_2 lies in the UV-ray region of the solar spectrum.[15] Figure 5 shows the spectrograms of UV-ray transmitting through different fabrics. The UPF values were calculated and are listed in Table IV.

From Figure 5, it is apparent that the three fabrics did not differ considerably in UV-ray transmittance in the wavelength range of 200–280 nm (UV-C region). But in the UV-A and UV-B regions, that is, in the wavelength range of 280–400 nm, the UV-ray transmittance of the PET/nano-TiO_2 fabrics (curves b and c) decreased steeply in contrast to that in pure PET fabric. It can be seen from Table IV that the transmittance of pure PET fabric was only 3.4% in the UV-B region, that is, the pure PET fabric exhibited good UV-B protection. When a low TiO_2 content was added to PET, for example, 1 wt %, the transmittance of PET fabric in the UV-B region was decreased to 0.4%. It

TABLE III
Crystallinity of PET Fiber with Different Nano-TiO_2 Contents

Content of nano-TiO_2 (%)	Crystallinity (%)
0	65.12%
1	61.74%
2	63.00%

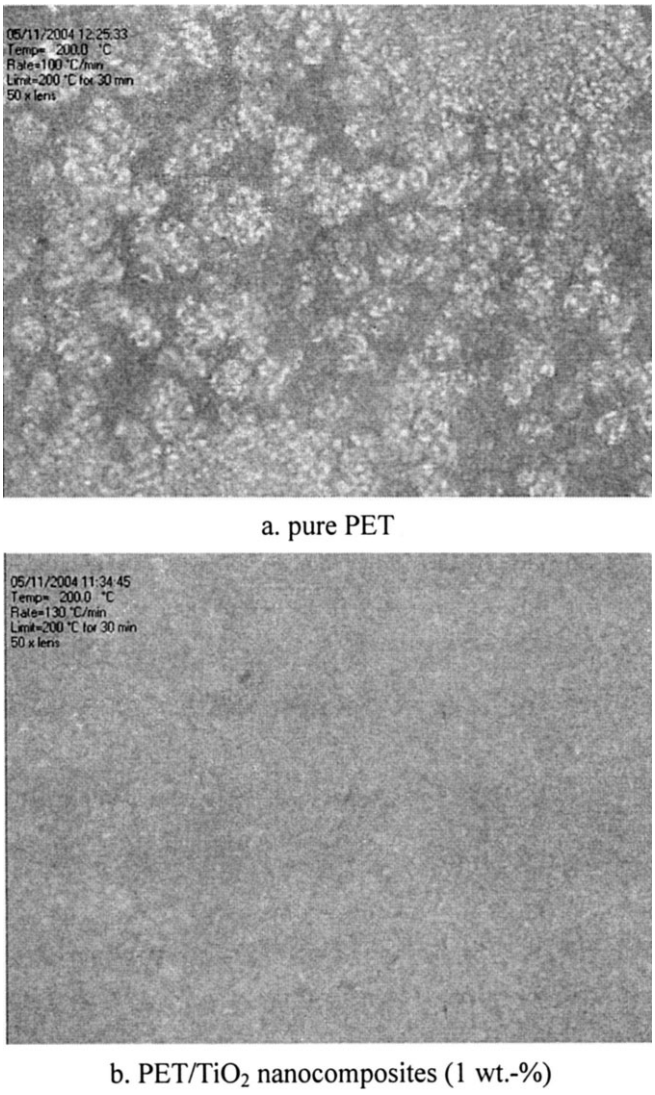

Figure 4 Polarizing microscope images of crystallization of different samples.

TABLE IV
The Average Transmittance of UV-ray and UPF Values of Different Fabrics

Content of nano TiO_2 (wt. %)	Average transmittance (%)		
	315–400 nm	280–315 nm	UPF
0	34.9	3.4	12
1	6.6	0.4	>50
2	4.8	0.3	>50

was noted that the transmittance of PET/nano-TiO_2 fabrics (1 wt %) in the UV-A region was sharply decreased from 34.9% to 6.6%, and its UPF value was above 50. According to AS/NZS 4399:1996, PET/nano-TiO_2 fabrics with low TiO_2 content exhibited excellent UV radiation protection.

To compare the effect of nano- and micro-TiO_2 on the UV-blocking property of PET fabrics, the UV-ray transmittance of PET fabrics with the same total TiO_2 content (0.8 wt %) and different nano-TiO_2 contents was determined and is plotted in Figure 6, which suggests that two samples exhibited good UV-B protection. However, the UV-ray transmittance of PET fabric with 0.5 wt % nano-TiO_2 plus 0.3 wt % micro-TiO_2 in the UV-A region was lower than that of PET fabric with 0.3 wt % nano-TiO_2 plus 0.5 wt % micro-TiO_2. From this, it could be concluded that TiO_2 nanoparticles could improve the UV-blocking property of PET fabrics remarkably in comparison with micro-TiO_2, although some TiO_2 nanoparticles aggregated in the PET matrix.

CONCLUSIONS

PET/TiO_2 nanocomposites prepared by *in situ* polymerization exhibited good UV radiation protection

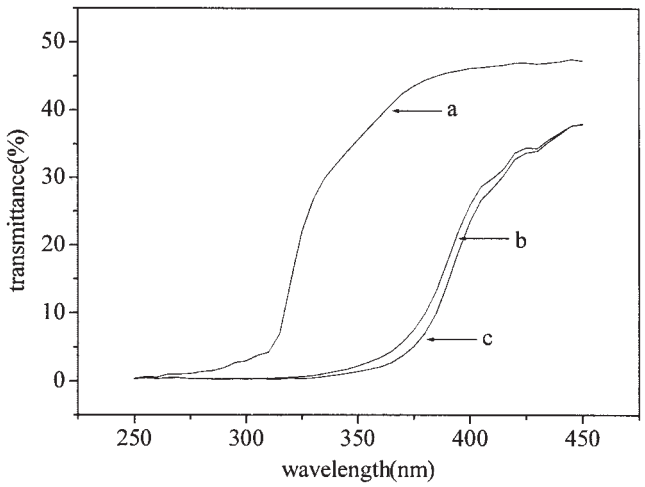

Figure 5 Spectrograms of UV-ray transmitting through different fabrics: (a) pure PET, (b) 1 wt % nano-TiO_2, (c) 2 wt % nano-TiO_2.

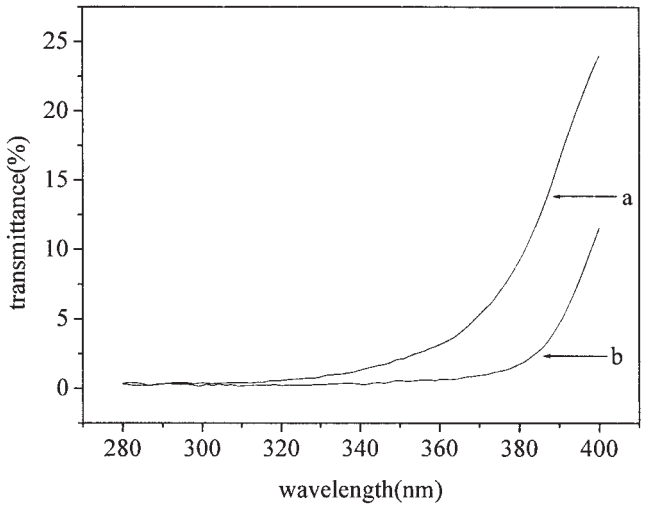

Figure 6 Spectrograms of UV-ray transmitting through different PET fabrics: (a) 0.3% nano-TiO_2 + 0.5% micro-TiO_2, (b) 0.5% nano-TiO_2 + 0.3% micro-TiO_2.

because of the high refractive index and absorption of UV light of rutile TiO_2. In this study, the uniform dispersion of TiO_2 in the nanocomposites by this method was confirmed by TEM and SPM measurements. PET/nano-TiO_2 fiber was prepared using suitable spinning parameters. The tensile strength of PET fibers with low TiO_2 content decreased slightly in contrast to that of pure PET fiber; at the same time it had a lower elongation at break. The UV-blocking property of the PET/nano-TiO_2 fiber improved remarkably, even at a very low nanorutile content. Its UPF value could reach above 50.

References

1. Phillips, R. Sources and Applications of Ultraviolet Radiation; Academic Press: London, 1983.
2. Hilfiker, R.; Kaufmann, W.; Reinert, G.; Sdhmidt, E. Text Res J 1996, 66(2), 61.
3. Xin, J. H.; Daoud, W. A.; Kong, Y. Y. Text Res J 2004, 74(2), 97.
4. AS/NZS 4399, Sun Protective Clothing Evaluation and Classification. Published jointly by Standards Australian and Standards New Zealand, 1996.
5. Murray, C. B.; Norris, D. J.; Bawendi, M. G. J Am Chem Soc 1993, 115, 8706.
6. Reddy, M. K.; Manorama, V. S.; Reddy, R. A. Mater Chem Phys 2003, 78, 239.
7. Nussbaumer, J. R.; Caseri, R.; Smith, P.; Tervoort, T. Macromol Mater Eng 2003, 288, 44.
8. Zhang, Q.; Gao, L.; Guo, J. Appl Catal B 2000, 26, 207.
9. Juangvanich, N.; Mauritz, K. A. J Appl Polym Sci 1998, 67, 1799.
10. McNally, T.; Murphy, R. W.; Lew, Y. C.; Turner, J. R.; Brennan, P. G. Polymer 2003, 44, 2761.
11. Lantelme, B.; Dumon, M.; Mai, C.; Pascault, J. P. J Non-Crystalline Solids 1996, 194(1), 63.
12. Li, Y.; Yu, J.; Guo, Z. Polym Int 2003, 52, 981.
13. Chang, J.; Kim, S. Polymer 2004, 45, 919.
14. Shen, L.; Du, Q.; Wang, H.; Zhong, W.; Yang, Y. Polym Int 2004, 53, 1153.
15. Zhang, Y.; Xiong, G.; Yao, N.; Yang, W.; Fu, X. Catal Today 2001, 68, 89.